

DESY 01-224
December 2001

Signatures of Supersymmetry in B Decays - A Theoretical Perspective

A. Ali

Deutsches Elektronen-Synchrotron DESY, Hamburg
Notkestraße 85, D-22603 Hamburg, FRG

Invited Talk; to be published in the Proceedings of the
International Conference on Flavor Physics ICFP2001,
Zhang-Jia-Jie City, Hunan Province, Peoples Republic of China,
May 31 – June 6, 2001.

Signatures of Supersymmetry in B Decays - A Theoretical Perspective

A. ALI

*Deutsches Elektronen-Synchrotron DESY, Notkestraße 85
D-22603 Hamburg, Germany
E-mail: ali@mail.desy.de*

We discuss precision tests of the standard model in radiative and semileptonic rare B -decays and CP-violating asymmetries, and possible signatures of supersymmetry in these processes. Motivated by current data, and with an eye on the forthcoming measurements, we restrict ourselves to the processes in which the benchmarks set by the standard model have either been met by ongoing experiments or are expected to be met shortly. This includes the mixing-induced CP asymmetry, measured through $\sin 2\beta$, and branching ratios for the radiative and semileptonic rare decays $B \rightarrow X_s \gamma$, $B \rightarrow K^* \gamma$, $B \rightarrow X_s \ell^+ \ell^-$ and $B \rightarrow (K, K^*) \ell^+ \ell^-$, where $\ell^\pm = e^\pm, \mu^\pm$.

1 Introduction

Experimental B physics is making big strides, thanks largely to the superb performance of the KEK and SLAC B factories and the BELLE and BABAR detectors, but also due to the solid foundation provided by CLEO, the LEP and SLC experiments, and by the CDF collaboration. The rich harvest of new experimental results includes the first measurements of CP violation in the B -meson system B_d^0 and \overline{B}_d^0 , involving statistically significant results by the BABAR¹ and BELLE² collaborations. The CP asymmetry in question, $a_{J\psi K_s}$, is measured through the time-dependent difference in the decay rates for $B_d^0 \rightarrow J/\psi K_s$ and its CP-conjugate process $\overline{B}_d^0 \rightarrow J/\psi K_s$ (as well as a number of other related final states such as $\psi(2S)K_s$, $J/\psi K_L$ etc.). Data on this asymmetry, allowing a clean determination of $\sin 2\beta$ (where β is one of the angles of the unitarity triangle UT), is now quantitative and can be meaningfully compared with the standard model (SM) predictions of the same. Likewise, it can be used to put constraints on additional CP-violating phases in beyond-the-SM (BSM) scenarios and we will illustrate this in terms of an additional phase, called θ_d , in the context of a supersymmetric theory.

Equally interesting from the point of view of precision tests of the SM and searches of BSM physics are a number of flavour-changing-neutral-current (FCNC) processes, of which the decay $b \rightarrow s \gamma$ is so far the most significant^{3,4,5,6}. Here also, SM has not only survived a rather crucial experimental test involving quantum (loop) effects in the FCNC sector, it has done so with a comfortable ease^{7,8,9}. Experiments at the B factories are about

to cross (or, have probably already crossed) the next milestone in rare B -decays, involving semileptonic FCNC decays. We have in mind here the decays $B \rightarrow (X_s, K^*, K)\ell^+\ell^-$, where the current experimental limits^{10,11,12} are fast approaching the SM-sensitivity^{13,14,15}. In fact in the decays $B \rightarrow K\ell^+\ell^-$, $\ell = e, \mu$, first measurements by the BELLE collaboration¹¹ are at hand, though the BABAR collaboration¹² still does not see any signal in this channel. So, more data is needed, which luckily is on its way. The next experimental milestone in this field will be reached with the measurement of the inclusive decays $B \rightarrow X_s\ell^+\ell^-$, since the SM-theory is now quantitative, in particular in the low dilepton invariant mass region^{15,16,17}. Data can be used to extract effective Wilson coefficients in a general theoretical scenario which we shall discuss, drawing heavily from a recent analysis¹⁵.

2 Constraints on $\sin 2\beta$ and an additional CP-violating phase θ_d

As is by now folk-lore, the measurement of $a_{J\psi K_s}$ yields $\sin 2\beta$ in the SM. The current experimental value of this quantity (including a scale factor in conformity with the Particle Data Group prescription) is $\sin 2\beta = 0.79 \pm 0.12$, and is now dominated by the BABAR¹ ($\sin 2\beta = 0.59 \pm 0.14(\text{stat}) \pm 0.05(\text{syst})$), and the BELLE² ($\sin 2\beta = 0.99 \pm 0.14(\text{stat}) \pm 0.06(\text{syst})$) measurements. SM-predictions of $\sin 2\beta$ based on indirect measurements of the sides of the unitarity triangle lie in the range $\sin 2\beta = 0.6 - 0.8$ ¹⁸. From this, we tentatively conclude that the current experiments and SM are in reasonable agreement with each other in $\sin 2\beta$. However, this *rapport* will be tested very precisely in future and it is sensible to estimate the magnitude of a BSM-phase allowed by current data.

In popular extensions of the SM, such as the minimal supersymmetric standard model (MSSM), one anticipates supersymmetric contributions to FCNC processes, in particular ΔM_{B_d} , ΔM_{B_s} (the mass differences in the B_d^0 - \overline{B}_d^0 and B_s^0 - \overline{B}_s^0 systems), and ϵ_K , characterizing the mixing-induced CP-asymmetry $\mathcal{A}_{\text{CP}}^{\text{mix}}$ in the K^0 - \overline{K}^0 system. However, if the Cabibbo-Kobayashi-Maskawa (CKM) matrix remains effectively the only flavour changing (FC) structure, which is the case if the quark and squark mass matrices can be simultaneously diagonalized, and all other FC interactions are associated with rather high scales, then all hadronic flavour transitions can be interpreted in terms of the same unitarity triangles which one encounters in the SM. In particular, in these theories $a_{\psi K_s}$ measures the same quantity $\sin 2\beta$ as in the SM. These models, usually called the minimal flavour violating (MFV) models¹⁹, are structured so that the SUSY contributions to ΔM_{B_d} , ΔM_{B_s} , and ϵ_K have the same CKM-dependence as the SM top quark contributions in the box diagrams

(denoted below by C_1^{Wtt}). Hence, supersymmetric effects for the UT-analysis can be effectively incorporated in terms of a single common parameter f by the following replacement²⁰:

$$\epsilon_K, \Delta M_{B_s}, \Delta M_{B_d}, a_{\psi K_S} : C_1^{Wtt} \rightarrow C_1^{Wtt}(1+f) . \quad (1)$$

The parameter f is positive definite and real, implying that there are no new phases in any of the quantities specified above. The size of f depends on the parameters of the supersymmetric models. Given a value of f , the CKM unitarity fits can be performed in these scenarios much the same way as they are done for the SM. Qualitatively, the CKM-fits in MFV models yield the following pattern for the three inner angles of the UT:

$$\beta^{\text{MFV}} \simeq \beta^{\text{SM}} ; \quad \gamma^{\text{MFV}} < \gamma^{\text{SM}} ; \quad \alpha^{\text{MFV}} > \alpha^{\text{SM}} , \quad (2)$$

and a recent CKM-fit along these lines yields the following central values for the three angles¹⁸:

$$\begin{aligned} f = 0 \text{ (SM)} : \quad & (\alpha, \beta, \gamma)_{\text{central}} = (95^\circ, 22^\circ, 63^\circ) , \\ f = 0.4 \text{ (MFV)} : \quad & (\alpha, \beta, \gamma)_{\text{central}} = (112^\circ, 20^\circ, 48^\circ) . \end{aligned} \quad (3)$$

leading to $(\sin 2\beta)_{\text{central}}^{\text{SM}} \simeq 0.70$ and $(\sin 2\beta)_{\text{central}}^{\text{MFV}} \simeq 0.64$. Thus, what concerns $\sin 2\beta$, the SM and the MFV models give similar results from the UT-fits, unless much larger values for the parameter f are admitted which are now unlikely due to the existing constraints on the MFV-SUSY parameters.

However, in a general extension of the SM, one expects that all the quantities appearing on the l.h.s. in Eq. (1) will receive independent additional contributions. In this case, the magnitude and the phase of the off-diagonal elements in the B_d^0 - \bar{B}_d^0 and B_s^0 - \bar{B}_s^0 mass matrices can be parametrized as follows^{21,22}:

$$\begin{aligned} M_{12}(B_d) &= \frac{\langle \bar{B}_d | H_{eff}^{\Delta B=2} | B_d \rangle}{2M_{B_d}} = r_d^2 e^{2i\theta_d} M_{12}^{\text{SM}}(B_d) , \\ M_{12}(B_s) &= \frac{\langle \bar{B}_s | H_{eff}^{\Delta B=2} | B_s \rangle}{2M_{B_s}} = r_s^2 e^{2i\theta_s} M_{12}^{\text{SM}}(B_s) . \end{aligned} \quad (4)$$

where r_d (r_s) and θ_d (θ_s) characterize, respectively, the magnitude and the phase of the new physics contribution to the mass difference ΔM_{B_d} (ΔM_{B_s}). It follows that a measurement of $a_{\psi K_S}$ would not measure $\sin 2\beta$, but rather a combination $\sin 2(\beta + \theta_d)$. In this scenario, one also expects new contributions in $M_{12}(K^0)$, bringing in their wake additional parameters (r_ϵ , θ_ϵ). They will alter the profile of CP-violation in the decays of the neutral kaons.

It is obvious that in such a general theoretical scenario, which introduces six *a priori* independent parameters, the predictive power vested in the CKM-UT analysis is lost. If the idea is to retain this predictivity, at least partially, then one has to work within a more limited framework. A model along these lines was introduced using the language of minimal insertion approximation (MIA)^{23,24} in a supersymmetric context. In this model²⁵, all FC transitions which are not generated by the CKM mixing matrix are proportional to the properly normalized off-diagonal elements of the squark mass matrices:

$$(\delta_{ij})_{AB}^{U,D} \equiv \frac{(M_{ij}^2)_{AB}^{U,D}}{M_{\tilde{q}_i} M_{\tilde{q}_j}} \quad (5)$$

where $i, j = 1, 2, 3$ and $A, B = L, R$. The dominant effect of the non-CKM structure contained in the MIA-parameters is to influence mainly the $b \rightarrow d$ and $s \rightarrow d$ transitions while the $b \rightarrow s$ transition is governed by the MFV-SUSY and the SM contributions alone. For what concerns the quantities entering in the UT analysis, the following pattern for the supersymmetric contributions emerges in this model:

$$\begin{aligned} \Delta M_{B_s} &: C_1^{Wtt} \rightarrow C_1^{Wtt}(1+f) & (6) \\ \epsilon_K, \Delta M_{B_d}, a_{\psi K_S} &: C_1^{Wtt} \rightarrow C_1^{Wtt}(1+f) + C_1^{MI} \equiv C_1^{Wtt}(1+f+g) & (7) \end{aligned}$$

where the parameters f and $g = g_R + ig_I$ represent normalized (w.r.t. the SM top quark Wtt) contributions from the MFV and MIA sectors, respectively. Hence, in the UT-analysis the contribution from the supersymmetric sector can be parametrized by two real parameters f and g_R and a parameter g_I , generating a phase θ_d , which is in general non-zero due to the complex nature of the appropriate mass insertion parameter. A precise measurement of $a_{\psi K_S}$ would fix this argument ($= \theta_d$).

The impact of the Extended-MFV model on the profile of the unitarity triangle in the $(\bar{\rho}, \bar{\eta})$ plane is shown in Fig. 1, which also shows the corresponding profiles in the SM and MFV models: the solid contour corresponds to the SM 95% C.L., the dashed one to a typical MFV case ($f = 0.4, g = 0$) and the dotted-dashed one to an allowed point in the Extended-MFV model ($f = 0, g_R = -0.2$ and $g_I = 0.2$). All three models give comparable fits. In Fig. 2 the CP asymmetry $a_{\psi K_S}$ is plotted as a function of $\arg \delta_{\tilde{u}_L \tilde{t}_2}$ (expressed in degrees). Here, $\delta_{\tilde{u}_L \tilde{t}_2}$ is a linear combination²⁴ of $(\delta_{13})_{LR}^U$ and $(\delta_{13})_{LL}^U$. The light and dark shaded bands correspond, respectively, to the SM and the experimental 1σ allowed regions. The solid line is drawn for $f = 0$ and $|g| = 0.28$. The experimental band flavours $\arg \delta_{\tilde{u}_L \tilde{t}_2}$ in the range $[0^\circ, 100^\circ]$. Employing

the explicit dependence

$$\theta_d = \frac{1}{2} \arg(1 + f + |g|e^{2i \arg \delta_{\bar{u}_L \bar{t}_2}}) \pmod{\pi}, \quad (8)$$

the above phase interval is translated into

$$-3^\circ < \theta_d < 8^\circ, \quad (9)$$

for the assumed values of $|g|$ and f , which is a typical range for θ_d for the small angle solution with the current values of $a_{\psi K_S}$.

Such a non-zero angle would have measurable consequences in $b \rightarrow d$ transitions^{25,26}, such as the isospin-violating ratio $\Delta^{\pm 0} = \frac{\Gamma(B^{\pm} \rightarrow \rho^{\pm} \gamma)}{2\Gamma(B^0(B^0) \rightarrow \rho^0 \gamma)} - 1$, and in direct CP-violating asymmetries $\mathcal{A}_{\text{CP}}(\rho^{\pm} \gamma) = \frac{\mathcal{B}(B^- \rightarrow \rho^- \gamma) - \mathcal{B}(B^+ \rightarrow \rho^+ \gamma)}{\mathcal{B}(B^- \rightarrow \rho^- \gamma) + \mathcal{B}(B^+ \rightarrow \rho^+ \gamma)}$, which may deviate measurably from their SM ranges. Recently, these quantities have been calculated in the SM by taking into account explicit $O(\alpha_s)$ corrections^{27,28}, using the so-called Large-Energy-Effective-Theory (LEET) approach²⁹. While there is considerable parametric uncertainty in the determination of $\mathcal{A}_{\text{CP}}(\rho^{\pm} \gamma)$ (and its analogue $\mathcal{A}_{\text{CP}}(\rho^0 \gamma)$), the estimates of $\Delta^{\pm 0}$ are quantitative. Testing these predictions should be feasible at the B factories in the next several years.

3 Inclusive Decay rate for $B \rightarrow X_s \gamma$ in the SM and SUSY

The effective Hamiltonian in the SM inducing the $b \rightarrow s \gamma$ transitions, obtained by integrating out the heavier degrees of freedom, can be expressed as follows:

$$\mathcal{H}_{\text{eff}} = -\frac{4G_F}{\sqrt{2}} V_{ts}^* V_{tb} \sum_{i=1}^8 C_i(\mu) O_i(\mu) \quad , \quad (10)$$

where G_F is the Fermi coupling constant and the CKM dependence has been made explicit; $O_i(\mu)$ are dimension-six operators at the scale μ , and $C_i(\mu)$ are the corresponding Wilson coefficients. Of these, the dominant operators are $\mathcal{O}_1 \sim (\bar{s}_L \gamma_\mu T^a q_L)(\bar{q}_L \gamma^\mu T^a b_L)$, $\mathcal{O}_2 \sim (\bar{s}_L \gamma_\mu q_L)(\bar{q}_L \gamma^\mu b_L)$, and the magnetic moment operators $\mathcal{O}_7 \sim (\bar{s}_L \sigma_{\mu\nu} b_R) F^{\mu\nu}$ and $\mathcal{O}_8 \sim (\bar{s}_L \sigma_{\mu\nu} b_R) T^a G^{a,\mu\nu}$, where $F^{\mu\nu}$ ($G^{a,\mu\nu}$) is the electromagnetic (chromomagnetic) field strength tensor, with T^a ($a = 1, \dots, 8$) being the SU(3) group generators. Current theoretical precision of the $b \rightarrow s \gamma$ decay rate is limited to $\mathcal{O}(\alpha_s)$, consisting of the anomalous dimension matrix in the next-to-leading order (NLO), the commensurate matching conditions, and the virtual and bremsstrahlung contributions. Also,

the leading power corrections in $1/m_b$ and $1/m_c$ have been calculated. The present experimental average of the branching ratio^{3,4,5,6}

$$\mathcal{B}(B \rightarrow X_s \gamma) = (3.22 \pm 0.40) \times 10^{-4}, \quad (11)$$

is in good agreement with the next-to-leading order prediction of the same in the SM, estimated as^{7,8} $\mathcal{B}(B \rightarrow X_s \gamma)_{\text{SM}} = (3.35 \pm 0.30) \times 10^{-4}$ for the pole quark mass ratio $m_c/m_b = 0.29 \pm 0.02$, rising to⁹ $\mathcal{B}(B \rightarrow X_s \gamma)_{\text{SM}} = (3.73 \pm 0.30) \times 10^{-4}$, if one uses instead the input value $m_c^{\overline{\text{MS}}}(\mu)/m_b^{\text{pole}} = 0.22 \pm 0.04$, where $m_c^{\overline{\text{MS}}}(\mu)$ is the charm quark mass in the $\overline{\text{MS}}$ -scheme, evaluated at a scale μ in the range $m_c < \mu < m_b$. The inherent uncertainty reflects the present accuracy of the theoretical branching ratio and the imprecise knowledge of the quark masses, in particular m_c and m_b . Precise measurements of the photon energy spectrum in $B \rightarrow X_s \gamma$ decays may help in decreasing some of these uncertainties.

The agreement between experiment and the SM for the $B \rightarrow X_s \gamma$ decay rate is quite impressive and this has been used to put non-trivial constraints on the BSM-physics, in particular supersymmetry^{30,8}. A recent analysis¹⁵ along these lines is discussed here for illustration. Following earlier works, the integrated $B \rightarrow X_s \gamma$ branching ratio can be solved as a function of the quantities $R_{7,8}(\mu_W) \equiv C_{7,8}^{\text{tot}}(\mu_W)/C_{7,8}^{\text{SM}}(\mu_W)$, where $R_{7,8}^{\text{tot}} = R_{7,8}^{NP} + R_{7,8}^{SM}$. Taking the scale $\mu_W = M_W$, for the purpose of the renormalization group evolution (RGE) also for the supersymmetric contributions, and imposing the experimental bound $\mathcal{B}(B \rightarrow X_s \gamma) = (3.22 \pm 0.40) \times 10^{-4}$, the corresponding allowed regions in the $[R_7(\mu_W), R_8(\mu_W)]$ plane are worked out. Evolving the allowed regions to the scale $\mu_b = 2.5$ GeV and assuming that new physics only enters in the effective Wilson coefficients $C_{7,8}$, the corresponding low-scale bounds in the plane $[R_7(2.5 \text{ GeV}), R_8(2.5 \text{ GeV})]$ are obtained, yielding

$$\begin{aligned} 0.785 \leq R_7(2.5 \text{ GeV}) \leq 1.255 &\Rightarrow -0.414 \leq C_7^{\text{tot}, < 0}(2.5 \text{ GeV}) \leq -0.259, \\ -1.555 \leq R_7(2.5 \text{ GeV}) \leq -1.200 &\Rightarrow 0.396 \leq C_7^{\text{tot}, > 0}(2.5 \text{ GeV}) \leq 0.513. \end{aligned} \quad (12)$$

Depending on the sign of C_7^{eff} , there are two allowed solutions - called C_7^{tot} -positive and C_7^{tot} -negative solutions. SM corresponds to the point $(R_7(\mu), R_8(\mu)) = (1, 1)$. Flavour-blind supersymmetric theories, such as SUGRA, allow points in the vicinity of the SM, though in a more general supersymmetric scenario, both C_7^{tot} -positive and C_7^{tot} -negative solutions are allowed³¹. These two scenarios can be distinguished, in principle, by measurements of the decays $B \rightarrow (X_s, K, K^*)\ell^+\ell^-$, which we discuss next.

4 Inclusive Decays $B \rightarrow X_s \ell^+ \ell^-$ in the SM and SUSY

The inclusive decays $B \rightarrow X_s \ell^+ \ell^-$ and the corresponding exclusive decays such as $B \rightarrow (K, K^*) \ell^+ \ell^-$ allow to get more detailed information on the flavour structure of the SM, and hence offer new search strategies for BSM physics. The effective Hamiltonian governing these decays in the SM is obtained by enlarging the sum given in Eq. (10) by the addition of two more terms involving the four-Fermi operators, denoted by \mathcal{O}_9 and \mathcal{O}_{10} :

$$\begin{aligned}\mathcal{O}_9 &\sim (\bar{s}_L \gamma_\mu b_L) \sum_\ell (\bar{\ell} \gamma^\mu \ell), \\ \mathcal{O}_{10} &\sim (\bar{s}_L \gamma_\mu b_L) \sum_\ell (\bar{\ell} \gamma^\mu \gamma_5 \ell),\end{aligned}\tag{13}$$

weighted, respectively, by the corresponding Wilson coefficients $C_9(\mu)$ and C_{10} . In most supersymmetric theories, the SM basis is sufficient to describe the generic transitions $b \rightarrow s \gamma$ and $b \rightarrow s \ell^+ \ell^-$, and we shall confine ourselves to discussing some possible BSM effects in this context.

Experimentally, the goal is to precisely measure a number of differential distributions, of which the dilepton invariant mass spectrum and the forward-backward asymmetry of the charged leptons in the dilepton rest frame are the best studied theoretically. BSM physics could manifest itself through additional contributions in the Wilson coefficients, shifting their values from the ones in the SM. This will lead to possible distortions in the two mentioned decay distributions, as well as some others not discussed for lack of space. From a theoretical point of view, inclusive decays $B \rightarrow X_s \ell^+ \ell^-$ are more robust, in particular in the dilepton mass region below the J/ψ resonance, as the explicit $\mathcal{O}(\alpha_s)$ improvements in the dilepton invariant mass distributions are now available in this region. Furthermore, the long-distance contributions, implemented through the matrix elements of the operators \mathcal{O}_1 and \mathcal{O}_2 , can be brought under control by a judicious choice of the experimental cuts, or estimated theoretically^{13,32}.

The dilepton invariant mass distribution for the inclusive decay $B \rightarrow X_s \ell^+ \ell^-$ can be written as

$$\begin{aligned}\frac{d\Gamma(b \rightarrow X_s \ell^+ \ell^-)}{d\hat{s}} &= \left(\frac{\alpha_{em}}{4\pi}\right)^2 \frac{G_F^2 m_{b,pole}^5 |V_{ts}^* V_{tb}|^2}{48\pi^3} (1 - \hat{s})^2 \times \\ &\left((1 + 2\hat{s}) \left(|\tilde{C}_9^{\text{eff}}|^2 + |\tilde{C}_{10}^{\text{eff}}|^2 \right) + 4(1 + 2/\hat{s}) |\tilde{C}_7^{\text{eff}}|^2 + 12\text{Re} \left(\tilde{C}_7^{\text{eff}} \tilde{C}_9^{\text{eff}*} \right) \right).\end{aligned}\tag{14}$$

The effective Wilson coefficients \tilde{C}_7^{eff} , \tilde{C}_9^{eff} and $\tilde{C}_{10}^{\text{eff}}$, including explicit $\mathcal{O}(\alpha_s)$ corrections, have been calculated^{15,16,17}.

The dilepton invariant mass distribution for the process $B \rightarrow X_s e^+ e^-$ calculated in NNLO is shown in Fig. 3 for the three choices of the scale $\mu = 2.5$ GeV, $\mu = 5$ GeV and $\mu = 10$ GeV (solid curves). In this figure, the left-hand plot shows the distribution in the very low invariant mass region ($\hat{s} \in [0, 0.05]$, with 0 to be understood as the kinematic threshold $s = 4m_e^2 \simeq 10^{-6}$ GeV², yielding $\hat{s} = 3.7 \times 10^{-8}$), and the right-hand plot shows the dilepton spectrum in the region beyond $\hat{s} > 0.05$, and hence this also holds for the decay $B \rightarrow X_s \mu^+ \mu^-$. It should be stressed that a genuine NNLO calculation only exists for values of \hat{s} below 0.25, which is indicated in the right-hand plot by the vertical dotted line. For higher values of \hat{s} , an estimate of the NNLO result is obtained by an extrapolation procedure discussed in detail elsewhere¹⁵. The so-called partial NNLO dilepton spectrum is also shown in each of these cases for the same three choices of the scale μ (dashed curves). Note that the NNLO dilepton invariant mass spectrum in the right-hand plot ($\hat{s} > 0.05$) lies below its partial NNLO counterpart, and hence the partial branching ratios for both the $B \rightarrow X_s e^+ e^-$ and $B \rightarrow X_s \mu^+ \mu^-$ decays are reduced in the full NNLO accuracy.

This framework has recently been used to calculate the branching ratio for $B \rightarrow X_s \ell^+ \ell^-$ in the SM, yielding¹⁵

$$\mathcal{B}(B \rightarrow X_s e^+ e^-) = (6.9 \pm 1.0) \times 10^{-6} \quad (\delta\mathcal{B}_{X_s ee} = \pm 15\%), \quad (15)$$

$$\mathcal{B}(B \rightarrow X_s \mu^+ \mu^-) = (4.2 \pm 0.7) \times 10^{-6} \quad (\delta\mathcal{B}_{X_s \mu\mu} = \pm 17\%). \quad (16)$$

The theoretical errors shown are obtained by estimating the errors from the individual input parameters, and the details can be seen in the original work. Current experimental data sees no signal for these decays, yielding the following upper limits⁴⁰

$$\mathcal{B}(B \rightarrow X_s \mu^+ \mu^-) \leq 19.1 \times 10^{-6} \text{ at } 90\% \text{ C.L.}, \quad (17)$$

$$\mathcal{B}(B \rightarrow X_s e^+ e^-) \leq 10.1 \times 10^{-6} \text{ at } 90\% \text{ C.L.}. \quad (18)$$

Thus, the current experimental sensitivity is typically a factor 3 away from the SM-estimates.

We now turn to the modifications of the effective Wilson coefficients \tilde{C}_7^{eff} , \tilde{C}_9^{eff} and $\tilde{C}_{10}^{\text{eff}}$ in the presence of new physics which modifies the Wilson coefficients C_7 , C_8 , C_9 and C_{10} at the matching scale μ_W . For lack of complete NLO calculations, we assume that only the lowest non-trivial order of these Wilson coefficients get modified by new physics, which means that $C_7^{(1)}(\mu_W)$, $C_8^{(1)}(\mu_W)$, $C_9^{(1)}(\mu_W)$, $C_{10}^{(1)}(\mu_W)$ get only indirectly modified. The shifts of the Wilson coefficients at the scale μ_W can be written as ($i = 7, \dots, 10$):

$$C_i(\mu_W) \longrightarrow C_i(\mu_W) + \frac{\alpha_s}{4\pi} C_i^{NP}(\mu_W). \quad (19)$$

These shift at the matching scale are translated through the RGE step into modifications of the coefficients $C_i(\mu_b)$ at the low scale μ_b . The bounds implied by the experimental results given in Eq. (18) (being the more stringent of the two limits) have been computed in the $[C_9^{NP}(\mu_W), C_{10}^{NP}]$ plane¹⁵. We shall show the cumulative bounds resulting from the combined analysis of all the inclusive and exclusive semileptonic decay in the next section.

5 Exclusive Decays $B \rightarrow K^*\gamma$ and $B \rightarrow K^*\ell^+\ell^-$ in the SM and Supersymmetry

Concentrating first on the transitions $B \rightarrow K^*\gamma^{(*)}$, with a real or virtual photon, the general decomposition of the matrix elements on all possible Lorentz structures present in the effective Hamiltonian admits seven form factors, which for the dilepton final state are functions of the momentum squared q^2 transferred from the heavy meson to the light one. When the energy of the final light meson E is large (the large recoil limit), one can expand the interaction of the energetic quark in the meson with the soft gluons in terms of Λ_{QCD}/E . Using HQET for the interaction of the heavy b -quark with the gluons, one can derive non-trivial relations between the soft contributions to the form factors²⁹. The resulting theory (LEET) reduces the number of independent form factors from seven in the $B \rightarrow K^*\gamma^*$ transitions to two in this limit. The relations among the form factors in the symmetry limit are broken by perturbative QCD radiative corrections arising from the vertex renormalization and the hard spectator interactions³³. To incorporate both types of QCD corrections, a factorization formula for the heavy-light form factors at large recoil is useful³³:

$$f_k(q^2) = C_{\perp k} \xi_{\perp} + C_{\parallel k} \xi_{\parallel} + \Phi_B \otimes T_k \otimes \Phi_{\rho}, \quad (20)$$

where $f_k(q^2)$ is any of the seven independent form factors in the $B \rightarrow K^*$ transitions at hand; ξ_{\perp} and ξ_{\parallel} are the two independent form factors remaining in the LEET-symmetry limit; T_k is a hard-scattering kernel calculated in $O(\alpha_s)$; Φ_B and Φ_{ρ} are the light-cone distribution amplitudes of the B - and ρ -meson convoluted with T_k ; $C_k = 1 + O(\alpha_s)$ are the hard vertex renormalization coefficients. An $O(\alpha_s)$ proof of the validity of Eq. (20) for radiative decays has, in the meanwhile, been provided by several groups^{27,28,34}, yielding

$$\begin{aligned} \mathcal{B}_{\text{th}}(B \rightarrow K^*\gamma) &= \tau_B \Gamma_{\text{th}}(B \rightarrow K^*\gamma) & (21) \\ &= \tau_B \frac{G_F^2 \alpha |V_{tb} V_{ts}^*|^2}{32\pi^4} m_{b,\text{pole}}^2 M^3 \left[\xi_{\perp}^{(K^*)} \right]^2 \left(1 - \frac{m_{K^*}^2}{M^2} \right)^3 \\ &\times \left| C_7^{(0)\text{eff}} + A^{(1)}(\mu) \right|^2, \end{aligned}$$

where $\alpha = \alpha(0) = 1/137$ is the fine-structure constant, M and m_{K^*} are the B - and K^* -meson masses, and τ_B is the lifetime of the B^0 - or B^+ -meson. The function $A^{(1)}$ in Eq. (21) lumps all three explicit $O(\alpha_s)$ contributions from the Wilson coefficient C_7^{eff} , $b \rightarrow s\gamma$ vertex, and the hard-spectator corrections to the $B \rightarrow K^*\gamma$ amplitude. NLO corrections yield a typical "K-factor" of 1.6, yielding²⁸

$$\begin{aligned} \mathcal{B}_{\text{th}}(B \rightarrow K^*\gamma) &\simeq (7.2 \pm 1.1) \times 10^{-5} \left(\frac{\tau_B}{1.6 \text{ ps}} \right) \left(\frac{m_{b,\text{pole}}}{4.65 \text{ GeV}} \right)^2 \left(\frac{\xi_{\perp}^{(K^*)}}{0.35} \right)^2 \\ &= (7.2 \pm 2.7) \times 10^{-5}, \end{aligned} \quad (22)$$

where the enlarged error in the second equation reflects the assumed error in the nonperturbative quantity, $\xi_{\perp}^{(K^*)}(0) = 0.35 \pm 0.07$. The estimates presented in Refs.^{34,27} are similar. The LEET-based estimates are larger than the experimental branching ratio for $B \rightarrow K^*\gamma$:

$$\begin{aligned} \mathcal{B}(B^{\pm} \rightarrow K^{*\pm}\gamma) &= (3.82 \pm 0.47) \times 10^{-5}, \\ \mathcal{B}(B^0(\bar{B}^0) \rightarrow K^{*0}(\bar{K}^{*0})\gamma) &= (4.44 \pm 0.35) \times 10^{-5}, \end{aligned} \quad (23)$$

though the attendant theoretical error, estimated as $\pm 40\%$, does not allow to draw a completely quantitative conclusion.

The price of agreement between the LEET approach and data can be specified in terms of the LEET-form factor $\xi_{\perp}^{(K^*)}(0)$. To that end, it is advantageous to calculate the following ratio of the exclusive to inclusive branching ratios:

$$R_{\text{exp}}(K^*\gamma/X_s\gamma) \equiv \frac{\bar{\mathcal{B}}_{\text{exp}}(B \rightarrow K^*\gamma)}{\bar{\mathcal{B}}_{\text{exp}}(B \rightarrow X_s\gamma)} = 0.13 \pm 0.02, \quad (24)$$

where the current experimental value of this ratio is also given, averaging over the charged and neutral B -decays. At NLO, the ratio $R(K^*\gamma/X_s\gamma)$ yields²⁸

$$\bar{\xi}_{\perp}^{(K^*)}(0) = 0.25 \pm 0.04, \quad \left[\bar{T}_1^{(K^*)}(0, \bar{m}_b) = 0.27 \pm 0.04 \right], \quad (25)$$

where $\bar{T}_1^{(K^*)}(0, \bar{m}_b)$ is the form factor in full QCD, determined using the quark masses in the \overline{MS} -scheme. This value is significantly smaller than the corresponding predictions from the QCD sum rules analysis^{14,35} $T_1^{(K^*)}(0) = 0.38 \pm 0.06$, and from the lattice simulations³⁶ $T_1^{(K^*)}(0) = 0.32_{-0.02}^{+0.04}$. The reason for this mismatch is not obvious and this point deserves further theoretical study.

In view of this, one can not insist that the absolute rates in exclusive decays can be calculated reliably in the LEET-approach. It should, however, be emphasized that any measurable CP asymmetry in the exclusive ($B \rightarrow K^*\gamma$) or inclusive ($B \rightarrow X_s\gamma$) decay will be a sure sign of BSM physics, as the SM CP asymmetry in either of these modes³⁷ is not expected to exceed $\frac{1}{2}\%$. Present experimental bounds on the CP asymmetry are³⁸ $\mathcal{A}_{\text{CP}}(B \rightarrow X_s\gamma) = (-0.079 \pm 0.018 \pm 0.022)$, and³⁹ $\mathcal{A}_{\text{CP}}(B \rightarrow K^{*0}\gamma) = (-0.035 \pm 0.094 \pm 0.012)$, obtained in the $K^+\pi^-$ mode. The first error in both cases is statistical and the second systematic. They still allow a lot of room for the BSM physics; however, not in the MFV and Extended-MFV models, discussed earlier.

5.1 $B \rightarrow K^*\ell^+\ell^-$ Decays

The NNLO corrections for $B \rightarrow X_s\ell^+\ell^-$ calculated by Bobeth et al.¹⁶ and by Asatrian et al.¹⁷ for the short-distance contribution have been recently harnessed¹⁵ to study the exclusive decays $B \rightarrow K^{(*)}\ell^+\ell^-$. This input is then combined with the form factors calculated with the help of the QCD sum rules¹⁴, ignoring the so-called hard spectator corrections, calculated in the decays $B \rightarrow K^*\ell^+\ell^-$ ³⁴. The rationale of this is the following: Beneke et al.³⁴ have shown that the dilepton invariant mass distribution in the low invariant mass region is rather stable against the explicit $O(\alpha_s)$ corrections, and the theoretical uncertainties are dominated by the form factors and other non-perturbative parameters specific to the large-energy factorization approach. As already discussed, current data on $B \rightarrow K^*\gamma$ decay yields typically a range $T_1(0) = 0.27 \pm 0.04$. To accommodate this, a value $T_1(0) = 0.33 \pm 0.05$, corresponding to the lower set of values in the QCD sum rules have been used in the NNLO analysis¹⁵, yielding

$$\mathcal{B}(B \rightarrow K\ell^+\ell^-) = (0.35 \pm 0.12) \times 10^{-6} \quad (\delta\mathcal{B}_{K\ell\ell} = \pm 34\%), \quad (26)$$

$$\mathcal{B}(B \rightarrow K^*e^+e^-) = (1.58 \pm 0.49) \times 10^{-6} \quad (\delta\mathcal{B}_{K^*ee} = \pm 31\%), \quad (27)$$

$$\mathcal{B}(B \rightarrow K^*\mu^+\mu^-) = (1.19 \pm 0.39) \times 10^{-6} \quad (\delta\mathcal{B}_{K^*\mu\mu} = \pm 33\%). \quad (28)$$

These estimates are lower than the NLO estimates¹⁴ due to two reasons: the explicit $O(\alpha_s)$ corrections lower the decay rates and the central values of the input form factors are also reduced so as to accommodate the $B \rightarrow K^*\gamma$ branching ratios in the same accuracy in $O(\alpha_s)$. They have to be confronted with the BELLE data¹¹ summarized below:

$$\mathcal{B}(B \rightarrow K\ell^+\ell^-) = (0.75_{-0.21}^{+0.25} \pm 0.09) \times 10^{-6}, \quad (29)$$

$$\mathcal{B}(B \rightarrow K^*\mu^+\mu^-) \leq 3.0 \times 10^{-6} \text{ at } 90\% \text{ C.L.}, \quad (30)$$

$$\mathcal{B}(B \rightarrow K^*e^+e^-) \leq 5.1 \times 10^{-6} \text{ at } 90\% \text{ C.L.} \quad (31)$$

Very recently, upper limits on these decays have been set by the BABAR collaboration, which at 90% C.L. are posted as¹²

$$\mathcal{B}(B \rightarrow K\ell^+\ell^-) \leq 0.50 \times 10^{-6}, \quad (32)$$

$$\mathcal{B}(B \rightarrow K^*\ell^+\ell^-) \leq 2.9 \times 10^{-6}, \quad (33)$$

where a ratio $\mathcal{B}(B \rightarrow K^*e^+e^-)/\mathcal{B}(B \rightarrow K^*\mu^+\mu^-) = 1.2$, following from the NLO QCD-SR estimate¹⁴ has been used to combine the $K^*e^+e^-$ and $K^*\mu^+\mu^-$ modes. As opposed to the BELLE collaboration, reporting a statistically significant signal in the $B \rightarrow K\ell^+\ell^-$ modes, BABAR data has no signal in this mode. However, the BABAR upper limit is not inconsistent with the BELLE measurement fluctuated down by slightly over a standard deviation.

To quantify the agreement between the SM and current data, we show the bounds implied by the experimental results given above in the $[C_9^{NP}(\mu_W), C_{10}^{NP}]$ plane. In Fig. 4, the bounds from the inclusive radiative decays and inclusive and exclusive semileptonic decays have been combined in a single plot. Note that the overall allowed region is driven by the constraints emanating from the decays $B \rightarrow X_s e^+e^-$ and $B \rightarrow K\ell^+\ell^-$. In showing the constraints from $B \rightarrow K\ell^+\ell^-$, we have used the BELLE measurement to get the following bounds:

$$0.37 \times 10^{-6} \leq \mathcal{B}(B \rightarrow K\ell^+\ell^-) \leq 1.2 \times 10^{-6} \text{ at 90\% C.L.}, \quad (34)$$

resulting in carving out an inner region in the $(C_9^{NP}(\mu_W), C_{10}^{NP})$ plane. The two plots shown in these figures correspond respectively to the C_7^{tot} -negative and C_7^{tot} -positive solutions discussed earlier. In Fig. 4 four regions are identified which are allowed by the constraints on the branching ratios that present very different forward-backward asymmetries. In Fig. 5 we show the shape of the FB asymmetry spectrum for the SM and other three sample points. The distinctive features are the presence or not of a zero and global sign of the asymmetry. A rough indication of the FB asymmetry behavior is thus enough to rule out a large part of the parameter space that the current branching ratios can not explore.

In order to explore the region in the $[C_9^{NP}, C_{10}^{NP}]$ plane (where $C_{9,10}^{NP}$ are the sum of MFV and MI contributions) that is accessible to these models, a high statistic scanning over the EMFV parameter space has been recently performed¹⁵ requiring each point to survive the constraints coming from the sparticle masses lower bounds and $b \rightarrow s\gamma$. The surviving points are shown in Fig. 4 together with the model independent constraints. Note that the region spanned by these points has been drastically reduced by the presence of the $b \rightarrow s\gamma$ constraint.

6 Summary

We summarize the main points of this talk.

- SM is in comfortable agreement with the measurements of the CP-asymmetry $a_{J/\psi}K_s$, yielding $\sin 2\beta$. However, current data also allows a BSM phase, with a typical range $-3^\circ < \theta_d < 8^\circ$.
- SM is also in comfortable agreement with data on $B \rightarrow X_s \gamma$. Due to the inherent two-fold ambiguity on the sign of the effective Wilson coefficient, both $C_7^{\text{tot}} > 0$ and $C_7^{\text{tot}} < 0$ solutions are allowed in supersymmetry involving different regions of the parameter space.
- Theoretical precision in exclusive decays is at present compromised by the imprecise knowledge of form factors and some other non-perturbative quantities. Ratios of the branching ratios, and some asymmetries (due to isospin-violations or CP-violation in $B \rightarrow \rho \gamma$ and $B \rightarrow K^* \gamma$) are more reliably calculable in this framework, and can be used to search for BSM physics. A quantitative test of the SM in these decays will be undertaken in inclusive decays $B \rightarrow X_s \ell^+ \ell^-$.
- Despite theoretical uncertainties, the experimental sensitivity on rare semileptonic B decays is already strong enough to provide non trivial bounds on the SUSY parameter space. Indeed, for the $C_7^{\text{tot}} > 0$ case, the larger portion of the SUSY allowed points is already ruled out.
- SUSY models can account only for a small part of the region allowed by the model independent analysis of current data. In the numerical analysis discussed here¹⁵, integrated branching ratios have been used to put constraints on the effective coefficients. They allow a multitude of solutions in the effective Wilson parameter space and can be disentangled from each other only with the help of both the dilepton mass spectrum and the forward-backward asymmetry in semileptonic rare B decays. Only such measurements would allow us to determine the exact values and signs of the Wilson coefficients C_7 , C_9 and C_{10} , also limiting C_8 and decipher the physics behind flavour transitions.

Acknowledgments

I would like to thank Cai-Dian Lü and Yue-Liang Wu for their warm hospitality during my stay in Beijing and at the ICFP 2001 conference.

References

1. B. Aubert *et al.* [BABAR Collaboration], Phys. Rev. Lett. **87** (2001) 091801 [hep-ex/0107013].
2. K. Abe *et al.* [BELLE Collaboration], Phys. Rev. Lett. **87** (2001) 091802 [hep-ex/0107061].
3. M. S. Alam *et al.* [CLEO Collaboration], Phys. Rev. Lett. **74** (1995) 2885.
4. S. Chen *et al.* [CLEO Collaboration], Phys. Rev. Lett. **87** (2001) 251807 [hep-ex/0108032].
5. R. Barate *et al.* [ALEPH Collaboration], Phys. Lett. **B429**, 169 (1998).
6. K. Abe *et al.* [BELLE Collaboration], Phys. Lett. B **511** (2001) 151 [hep-ex/0103042].
7. K. Chetyrkin, M. Misiak and M. Münz, Phys. Lett. B **400**, 206 (1997) [Erratum-ibid. B **425**, 414 (1997)] [hep-ph/9612313].
8. A. L. Kagan and M. Neubert, Eur. Phys. J. C **7**, 5 (1999) [hep-ph/9805303].
9. P. Gambino and M. Misiak, Nucl. Phys. B **611**, 338 (2001) [hep-ph/0104034].
10. K. Abe *et al.* [Belle Collaboration], BELLE-CONF-0110 [hep-ex/0107072].
11. K. Abe *et al.* [BELLE Collaboration], Phys. Rev. Lett. **88** (2002) 021801 [hep-ex/0109026].
12. B. Aubert *et al.* [BABAR Collaboration], Report BABAR-PUB-01/19; SLAC-PUB-9102 [hep-ex/0201008].
13. A. Ali, G. Hiller, L. T. Handoko and T. Morozumi, Phys. Rev. D **55**, 4105 (1997) [hep-ph/9609449].
14. A. Ali, P. Ball, L. T. Handoko and G. Hiller, Phys. Rev. D **61**, 074024 (2000) [hep-ph/9910221].
15. A. Ali, E. Lunghi, C. Greub and G. Hiller, Report DESY 01-217 [hep-ph/0112300].
16. C. Bobeth, M. Misiak and J. Urban, Nucl. Phys. B **574** (2000) 291 [hep-ph/9910220].
17. H. H. Asatrian, H. M. Asatrian, C. Greub and M. Walker, Phys. Lett. B **507** (2001) 162 [hep-ph/0103087];
H. H. Asatryan, H. M. Asatrian, C. Greub and M. Walker, [hep-ph/0109140].
18. See, for example, A. Ali and D. London, Eur. Phys. J. **C18**, 665 (2001), [hep-ph/0012155].
19. M. Ciuchini, G. Degrossi, P. Gambino, and G. F. Giudice, Nucl. Phys.

- B534**, 3 (1998), [hep-ph/9806308].
20. A. Ali and D. London, Eur. Phys. J. **C9**, 687 (1999), [hep-ph/9903535]. Phys. Rept. **320**, 79 (1999), [hep-ph/9907243].
 21. A. G. Cohen, D. B. Kaplan, F. Lepeintre, and A. E. Nelson, Phys. Rev. Lett. **78**, 2300 (1997), [hep-ph/9610252].
 22. J. P. Silva and L. Wolfenstein, Phys. Rev. **D55**, 5331 (1997), [hep-ph/9610208].
 23. L. J. Hall, V. A. Kostelecky, and S. Raby, Nucl. Phys. **B267**, 415 (1986).
 24. A. J. Buras, A. Romanino, and L. Silvestrini, Nucl. Phys. **B520**, 3 (1998), [hep-ph/9712398].
 25. A. Ali and E. Lunghi, Eur. Phys. J. C **21**, 683 (2001) [hep-ph/0105200].
 26. A. Ali, L. T. Handoko and D. London, Phys. Rev. D **63**, 014014 (2000) [hep-ph/0006175].
 27. S. W. Bosch and G. Buchalla, Nucl. Phys. B **621**, 459 (2002) [hep-ph/0106081].
 28. A. Ali and A. Y. Parkhomenko, Report DESY 01-068 [hep-ph/0105302].
 29. J. Charles, A. Le Yaouanc, L. Oliver, O. Pene and J. C. Raynal, Phys. Rev. D **60**, 014001 (1999) [hep-ph/9812358].
 30. J. L. Hewett and J. D. Wells, Phys. Rev. D **55**, 5549 (1997) [hep-ph/9610323].
 31. E. Lunghi, A. Masiero, I. Scimemi and L. Silvestrini, Nucl. Phys. B **568** (2000) 120 [hep-ph/9906286].
 32. G. Buchalla, G. Isidori and S. J. Rey, Nucl. Phys. B **511**, 594 (1998) [hep-ph/9705253].
 33. M. Beneke and T. Feldmann, Nucl. Phys. B **592**, 3 (2001) [hep-ph/0008255].
 34. M. Beneke, T. Feldmann and D. Seidel, Nucl. Phys. B **612**, 25 (2001) [hep-ph/0106067].
 35. P. Ball and V. M. Braun, Phys. Rev. D **58**, 094016 (1998) [hep-ph/9805422].
 36. L. Del Debbio, J. M. Flynn, L. Lellouch and J. Nieves [UKQCD Collaboration], Phys. Lett. B **416**, 392 (1998) [hep-lat/9708008].
 37. J. M. Soares, Nucl. Phys. B **367**, 575 (1991).
 38. T. Coan et al. [CLEO Collaboration], Phys. Rev. Lett. **86**, 5661 (2001) [hep-ex/0010075].
 39. A. Ryd et al. [BABAR Collaboration], Proc. Int. Symp. on Heavy Flavour Physics 9.

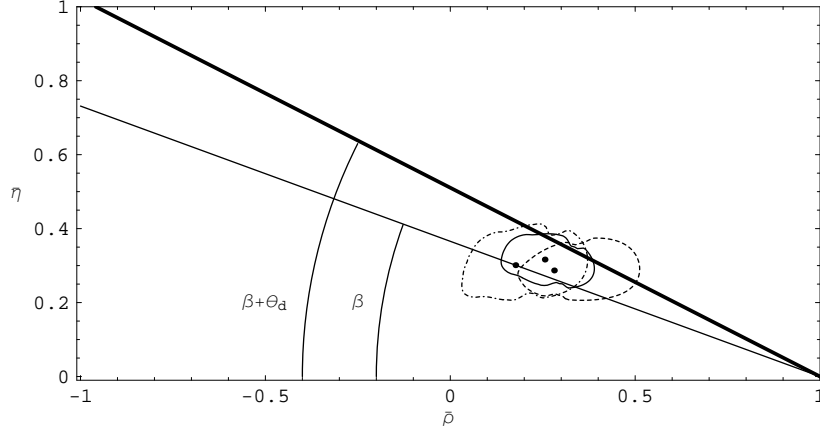


Figure 1: Allowed 95 % C.L. contours in the $(\bar{\rho}, \bar{\eta})$ plane. The solid contour corresponds to the SM case, the dashed contour to the Minimal Flavour Violation case with $(f = 0.4, g = 0)$ and the dashed-dotted contour to the Extended-MFV model discussed in the text $(f = 0, g_R = -0.2, g_I = 0.2)$. (From Ref. 25.)

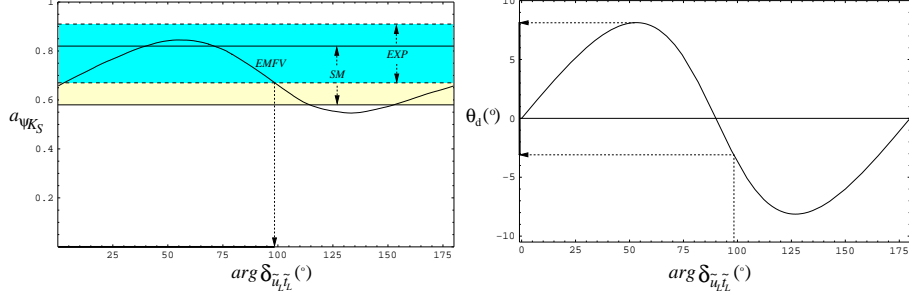


Figure 2: The CP asymmetry $a_{\psi K_S}$ as a function of $\arg \delta_{\bar{u}_L \bar{t}_2}$ expressed in degrees. The solid curve corresponds to the Extended-MFV model $(f = 0, |g| = 0.28)$. The light and dark shaded bands correspond, respectively, to the allowed 1σ region in the SM $(0.58 \leq a_{\psi K_S} \leq 0.82)$ and the current 1σ experimental band $(0.67 \leq a_{\psi K_S} \leq 0.91)$. The plot on the right shows the correlation between $\arg \delta_{\bar{u}_L \bar{t}_2}$ and the angle θ_d : $\theta_d = \frac{1}{2} \arg(1 + f + |g|e^{2i \arg \delta_{\bar{u}_L \bar{t}_2}})$, (mod π). The experimentally allowed region flavours $0^\circ < \arg \delta_{\bar{u}_L \bar{t}_2} < 100^\circ$ that translates into $-3^\circ < \theta_d < 8^\circ$. (From Ref. 25.)

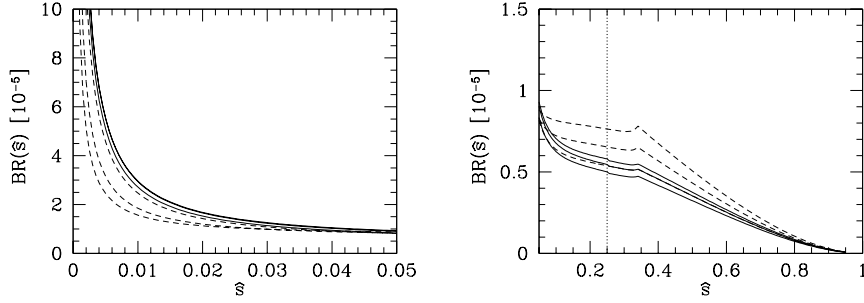


Figure 3: *Partial (dashed lines) vs full (solid lines) NNLO computation of the branching ratio $B \rightarrow X_s e^+ e^-$. In the left plot ($\hat{s} \in [0, 0.05]$) the lowest curves are for $\mu = 10$ GeV and the uppermost ones for $\mu = 2.5$ GeV. In the right plot the μ dependence is reversed: the uppermost curves correspond to $\mu = 10$ GeV and the lowest ones to $\mu = 2.5$ GeV. The right-hand plot also holds for the decay $B \rightarrow X_s \mu^+ \mu^-$. (From Ref. 15.)*

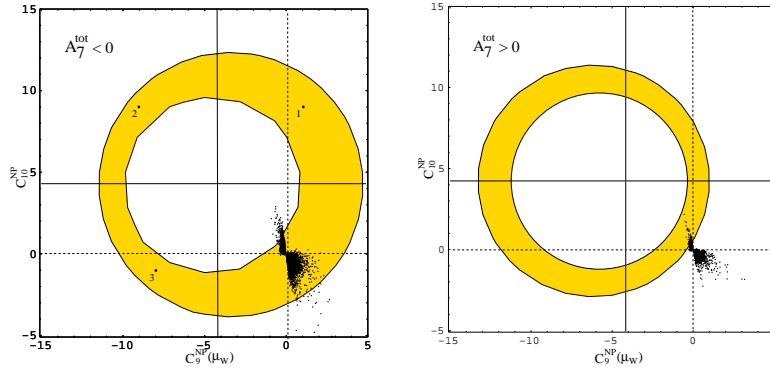


Figure 4: **NNLO Case.** *Superposition of all the constraints. The plots correspond to the $C_7^{\text{tot}}(2.5 \text{ GeV}) < 0$ and $C_7^{\text{tot}}(2.5 \text{ GeV}) > 0$ case, respectively. The points are obtained by means of a scanning over the EMFV parameter space and requiring the experimental bound from $B \rightarrow X_s \gamma$ to be satisfied. (From Ref. 15.)*

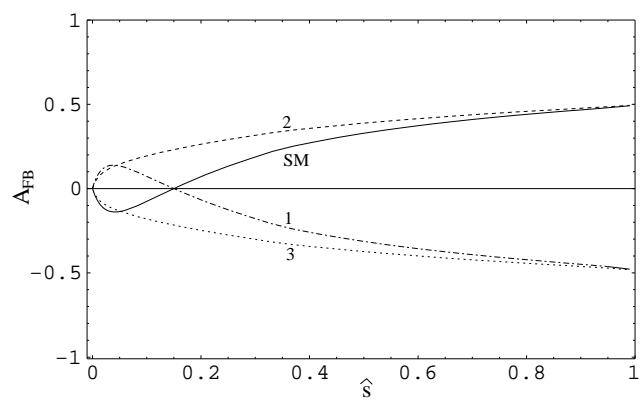


Figure 5: *Differential Forward-Backward asymmetry for the decay $B \rightarrow X_s \ell^+ \ell^-$. The four curves correspond to the points indicated in Fig. 4. (From Ref. 15.)*